

***E*WareNet: Emotion Aware Human Intent Prediction and Adaptive Spatial Profile Fusion for Social Robot Navigation**

Venkatraman Narayanan, Bala Murali Manoghar, Rama Prashanth RV and Aniket Bera
University of Maryland, College Park, USA

Abstract

We present *E*WareNet, a novel intent-aware social robot navigation algorithm among pedestrians. Our approach predicts the trajectory-based pedestrian intent from historical gaits, which is then used for intent-guided navigation taking into account social and proxemic constraints. To predict pedestrian intent, we propose a transformer-based model that works on a commodity RGB-D camera mounted onto a moving robot. Our intent prediction routine is integrated into a mapless navigation scheme and makes no assumptions about the environment of pedestrian motion. Our navigation scheme consists of a novel obstacle profile representation methodology that is dynamically adjusted based on the pedestrian pose, intent, and emotion. The navigation scheme is based on a reinforcement learning algorithm that takes into consideration human intent and robot's impact on human intent, in addition to the environmental configuration. We outperform current state-of-art algorithms for intent prediction from 3D gaits.

1. Introduction

Recent technological advancements are making human-robot collaborations increasingly important. This can have many applications, including autonomous driving, social robotics, and surveillance systems. As humans and robots co-inhabit space, designing robots that follow collision-free paths and are socially acceptable to humans is becoming increasingly important, creating several challenges. For example, in the case of a densely crowded street, the robot needs to foresee the movements of an oblivious walker who is unaware they are in its path for friendlier navigation. Understanding the emotional perceptions in such scenarios enables the robot to make more informed decisions and navigate in a socially-conscious manner.

The study of human emotions has been a much-researched subject in areas like psychology, human-robot collaboration, and interaction, etc. Certain studies have sought to identify the emotion in people based on cues such

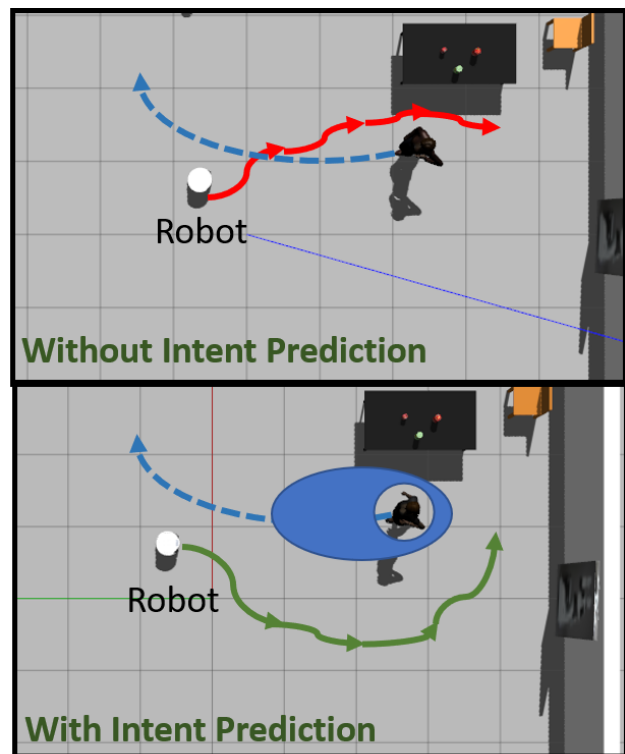


Figure 1. **E**wareNet: The top figure represents the path taken by the robot without intent prediction where the trajectory intercepts the path to be taken by the human. The bottom figure shows the path taken by the robot with the intent prediction pipeline where even though there is enough space and a shorter route is available, the robot takes a longer path giving enough personal space.

as body movement (walking style, etc.) [18, 25], and verbal cues (speech tonalities and patterns) [37, 36]. There are also multimodal approaches that utilize a combination of these cues to recognize the person's emotion [22, 7, 23]. A major challenge is combining information from the robot's sensors for effective navigation. Furthermore, the robot's awareness of uncertainty within the sensor suite and its adaptive nature to emerging situations is a demanding obstacle.

Several approaches have addressed a socially-acceptable

robot navigation problem. Many recent works like [25], [38], focuses on social robot navigation in crowded scenarios. However, these algorithms suffer from the following drawbacks:

1. They rely on emotionally reactive navigation planning, which means that the perceived emotions are based entirely on historical gait sequences and do not consider gait predictions of the future.
2. The influence of the robot’s behaviour on the emotional response of humans is not taken into account.
3. The proxemic constraints for humans are heuristically designed from psychology studies. While this works in most cases, it doesn’t efficiently capture each individual’s uniqueness in comfort space.

To overcome these challenges, we propose *EWareNet*, a novel algorithm for a real-time, gait-based, intent-aware robot navigation algorithm in crowded scenes that takes into account the pedestrian emotional state. *EWareNet* is designed to work with commercial off-the-shelf RGB-D cameras and depth sensors that can be retrofitted to moving platforms or robots for navigation. The **major contributions** of our work can be summarized as follows:

- We introduce a novel approach using *transformers/recurrent networks* to predict the full-body human intent or behavior in the form of trajectory/gaits based on historical gait sequences, which drastically improves accuracy compared to the state-of-the-art.
- We also present a novel navigation planning algorithm based on deep reinforcement learning that takes into consideration the environment, human intent, and the robot’s reactionary impact on human behavior.
- Our method explicitly considers pedestrian behavior in crowds and the robot’s impact on the environment.
- Finally, we introduce an adaptive spatial density function to represent the proximal constraints for humans that captures humans’ unique personal comfort space in terms of pose, intent, and emotion.

Human emotion and intent are very subjective and greatly influenced by many environmental and psychological factors. Therefore in this work, we focus only on the *perceived* emotions from the point of an external observer as opposed to *actual* internal emotion. We also predict human intent as a potential full-body future trajectory based upon historical trajectories/gait patterns for a more efficient navigation strategy and may not represent actual/hidden intent.

The paper is organized as follows: Section 2 presents related work, section 3 gives an overview of our pipeline

and describes each stage of our pipeline in detail, and finally in 4 we evaluate the results of our work.

2. Related Work

In this section, we present a brief overview of social-robot navigation algorithms. We also review related work on emotion modeling and classification from visual cues.

2.1. Intention Prediction

In social robotics, an accurate prediction of human trajectories plays a major role in robots’ decision in terms of reactive response, navigation planning etc. Human Intention Prediction is largely modeled as a trajectory prediction problem. Recurrent Neural Network based architectures are widely used for predicting the human trajectories [31, 27, 1]. [24] use a Graph Convolution method to predict the trajectories and showed that Temporal Graph Convolutions are much better at predicting the human trajectories compared to recurrent networks.

Most recurrent networks for trajectory prediction leverages some form of attention mechanism to improve the trajectories. [1, 31] uses a history of observed trajectories with either predicted future trajectory or location around humans to predict the intent. [27] provide skeletal joint kinematics as attention for trajectory prediction. These models one way or the other solely depend on trajectory and kinematics of joints for predicting the intent and there is no attention given to the emotion of the humans.

2.2. Social Robotics and Emotionally-Guided Navigation

There exists a substantial amount of research that focuses on identifying the emotions of humans based on body posture, movement, and other non-verbal cues. Ruiz-Garcia et al. [33] and Tarnowski et al. [35], use deep learning to classify different categories of emotion from facial expressions. [23] use multiple modalities such as facial cues, human pose and scene understanding. Randhavane et al. [28, 30] classify emotions into four classes based on affective features obtained from 3D skeletal poses extracted from human gait cycles. Their algorithm, however, requires a large number of 3D skeletal key-points to detect emotions and is limited to single individual cases. Bera et al. [3, 4] classify emotions based on facial expressions along with a pedestrian trajectory obtained from overhead cameras. Although this technique achieves good accuracy in predicting emotions from trajectories and facial expressions, it explicitly requires overhead cameras in its pipeline. [25] provide an end-to-end deep learning based emotion classification approach, that takes in skeletal gaits from arbitrary view. [11] modeled the navigation of a social robot based on human-robot trust interactions.

2.3. Proxemic Constraints Modeling

Usually, robots working in human environments have used navigation algorithms where all obstacles are considered of similar relevance, including people. [3] have studied the effects of comfort space of humans from a psychology perspective and showed that comfort space varies based on the emotion of humans. To avoid discomforting humans, social robots must consider them special entities, evaluating the people’s level of comfort with respect to the route of the robot. The navigation model of [3, 25] uses the predicted emotions and use a constant multiplier to maintain proper comfort space with the humans while planning the robot path.

Vega et al [38] proposed a human-aware navigation strategy based on space affordances. The method is built upon the use of an adaptive spatial density function that efficiently cluster groups of people according to their spatial arrangement. The paper [20] discusses deals with how an agent should learn the behavior from reward provided by a live human trainer rather than from the usual pre-coded reward function in a reinforcement learning framework. With designed CNN-RNN model, our analysis shows that telling trainers to use facial expressions and competition can improve the accuracies for estimating positive and negative feedback using facial expressions.

All these methods consider emotion as a constant metric for formulating proxemic constraints and do not adapt the navigation strategy with the change in the emotion of humans.

2.4. Sensor Fusion for Effective Navigation

LIDAR data is more robust in terms of depth prediction when compared to depth estimation from monocular depth camera. In our work we detect the humans and classify their emotion using RGBD images. This information has to be transferred to LIDAR data for an effective navigation. The approach described in [8] uses a deep learning model to carry out road detection by fusing LIDAR point clouds and camera images. An unstructured and sparse point cloud is first projected onto the camera image plane and then up-sampled to obtain a set of dense 2D images encoding spatial information. Several fully convolutional neural networks (FCNs) are then trained to carry out road detection, either by using data from a single sensor, or by using three fusion strategies: early, late, and the newly proposed cross fusion.

While this approach is very popular among people working with multi-sensor data, we observe that ours best work with projective geometry. We map camera frame to LiDAR frame using *intrinsic and extrinsic calibrations*. We believe that due to the complexities that accompany indoor setup, the fusion described in [8] fails for us.

3. Overview and Methodology

EWareNet is a novel algorithm for intent-aware socially-acceptable navigation through crowded scenarios. The human intentions are predicted based on 3D skeletal trajectories from an onboard RGB-D camera. The intent trajectories are then used by our navigation pipeline for socially-acceptable navigation. Our navigation planning is adaptive to the individual comfort space constraints of humans and to the uncertainty in the sensor suite of the robot. We use dynamic obstacle representation for humans, based on a Gaussian distribution to capture the individuality in comfort space constraints.

The following subsections will describe our approach in detail. We discuss the details of the datasets used for training our pipeline, along with the pre-processing techniques employed. Following this, we focus on our intent prediction routine, where we also discuss our human pose extraction from an RGB-D camera briefly. Finally, we discuss our navigation system.

3.1. Human Pose Extraction

An efficient human pose estimation algorithm is critical to our work. With that in mind, we use a robust system, described in [9], to extract the poses from humans walking in a crowded real-world scenario from an RGB-D camera. The system consists of a two-step network trained in a weakly supervised fashion. A *Structure-Aware PoseNet (SAP-Net)* provides an initial pose estimate based on spatial information of joint locations of people in the video. Later, a time-series *Temporal PoseNet (TP-Net)* corrects the initial estimate by adjusting illegal joint angles and joint distances. The temporal network also helps in tracking the human individual across the video frames. Hence, we have a set of temporally correct, *Human Joint Pose Sequence* for every human in the video as an output from the system.

3.2. Human Intent Prediction

Our Human Intent Prediction module is designed as a pose/trajectory prediction system, based on a set of skeletal gait sequences. The intent prediction system consists of three parts, (i) an *encoding transformer network*, (ii) *decoding transformer network*, and (iii) *emotion context mechanism*. Figure 2 provides a schematic representation of our Human Intent Prediction pipeline.

3.2.1 Emotion Context Network

Our emotion context network builds on [25]. It is a multi-view emotion classification network. The architecture takes in the gait sequences consisting of 16 joints (depicted in figure 2) for 75 time steps to classify them into one of 4 emotions (*Happy, Sad, Angry, Neutral*). The gait sequences

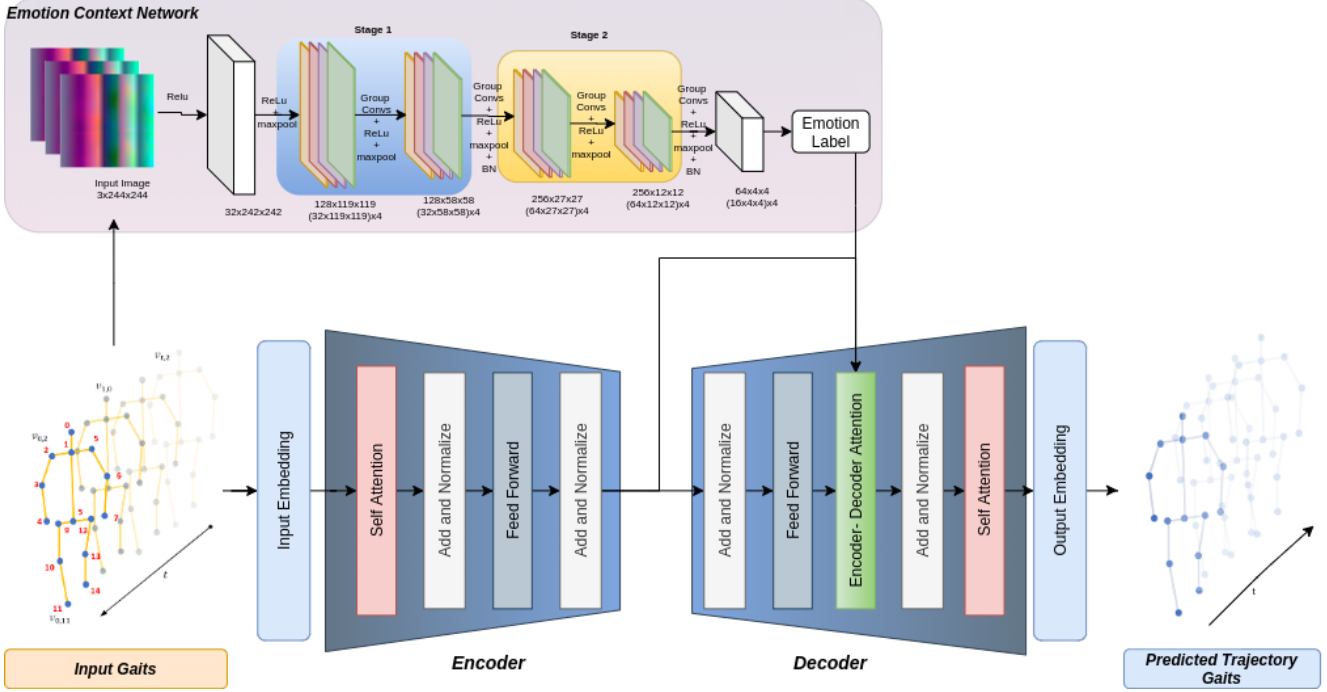


Figure 2. **Human Intent Prediction:** Our proposed method for prediction human intentions as full-body skeletal trajectory paths. It consists of a two-part network - (i) **Emotion Context Network** and **Encoding & Decoding Transformer Network**. The *Emotion Context Network* provides an additional **attention mechanism** on top of the self-attention mechanism in transformer networks.

are processed into image embeddings to leverage faster processing abilities of *Convolution Neural Networks* [25]. The embedded images are fed to the classification network. The classification network (*ECN*) consists of multiple layers of grouped convolutions. The grouped convolutions aids in classifying the emotions for different camera angle view groups. The extracted emotion is fed as an attention mechanism to our *Transformer Network* to obtain intent-aware trajectory predictions.

$$e_i = ECN(I_i) \quad (1)$$

Each gait sequences (i) is assigned an emotion label, (e_i), based on equation 1, where *ECN* represents the emotion classification network, I_i , represents the image embedding of the gait sequences i

3.2.2 Encoding and Decoding Transformer Net

The transformer (TF) network predicts the intent-aware future full-body gait trajectories for every human based on the historical gaits. The transformer networks have been successfully used to produce state-of-the-art results involving time-series sequences. They have been used in NLP tasks [10, 6] and time-series forecasting [21]. Guiliari et al. [13] uses transformer networks to generate state-of-the-art results on pedestrian trajectory prediction. Our trajectory prediction network is inspired by transformer networks for

its superiority over other recurrent neural network models [13] for time-series tasks.

$$e_{i,t} = G_{i,t}^T \cdot W_g \quad (2)$$

The input gait sequences for each human, $G_{i,t}$, are fed to a linear encoding layer given by equation 2. The embedded gaits inputs are fed to the transformer network. Transformer (TF) network is a modular architecture (figure 2). It consists of an encoder and the decoder networks composed of 6 layers, with three building blocks each: (i) an self-attention module, (ii) a feed-forward fully-connected module, and (iii) two residual connections after each of the previous blocks. The self-attention modules within the TF net provide the capability to capture non-linearities in the trajectory.

The encoder model creates a representation, $E_s^{(i,t)}$, of the input gait sequences, forming a memory module. The encoder representation is utilized by the decoder model to auto-regressively predicts future trajectories.

The *encoder-decoder attention* layer of decoder network is fed with encoder representation and emotion context from emotion context network in 3.2. The emotion context remains constant for all the timesteps predicted by the decoder. The intent-aware trajectory predictions are used in our navigation pipeline.

3.3. Proxemic Constraints Modeling

The personal space constraints are derived from many psychology works [32]. Personal space constraints are very important in social robotics, and emotion-guided navigation [17]. The comfort space constraints defined in [19], [32] describe the social norms that the robot must consider to not cause discomfort to people around it. The comfort space constraints described in [32], [19], [25] does not consider the individuality of humans. Our method strives to capture the comfort space individuality among pedestrians.

Our human personal space modeling is an adaptive spatial density function, similar to [38]. In an arbitrary global map in space, a human, i , is represented by position, orientation and emotion (from 3.2.1), $h_i = (x_i, y_i, \theta_i, C_i)^T$. Here (x_i, y_i) represents the position of the human, θ_i represents the orientation, and C_i represents the comfort space derived from emotion. The position coordinates from each human will be derived from the LiDAR coordinates after mapping detected humans from the camera frame to the LiDAR frame using projective geometry. The orientation and emotion are derived from section 3.2.1. The view-group angle predicted by the model is used as the approximated orientation. The gaussian expression for personal space is defined by equation 3.

$$g_{h_i} = C_i * \exp(-k_1(x - x_i)^2 + k_2(x - x_i)(y - y_i) + k_3(y - y_i)^2) \quad (3)$$

Here, C_i is the comfort space multiplier given by,

$$C_i = \frac{\sum_{j=1}^4 c_j \cdot \max(e_j)}{\sum_{j=1}^4 e_j} \cdot v_g \quad (4)$$

where, e_j represents a column vector of the emotion context output from section 3.2.1, which corresponds to the group outcomes for each individual emotion. c_j is an individual's comfort space constant derived from psychological experiments described in [32], chosen from a set $\{90.04, 112.71, 99.75, 92.03\}$ corresponding to the comfort spaces (radius in cm) for $\{happy, sad, angry, neutral\}$ respectively. These distances are based on how comfortable pedestrians are while interacting with others. v_g is a view-group constant chosen from a set of $\{1, 0.5, 0, 0.5\}$ based on the view group g , defined in [25].

Also, k_1, k_2, k_3 in equation 3 are the coefficients taking into account the orientation $\theta_i \in [0, 2\pi)$, defined in equations 5, 6, 7.

$$k_1(\theta_i) = \frac{\cos(\theta_i^2)}{2\sigma^2} + \frac{\sin(\theta_i^2)}{2\sigma_s^2} \quad (5)$$

$$k_2(\theta_i) = \frac{\sin(2\theta_i)}{4\sigma^2} \frac{\sin(2\theta_i)}{4\sigma_s^2} \quad (6)$$

$$k_3(\theta_i) = \frac{\sin(\theta_i^2)}{2\sigma^2} + \frac{\cos(\theta_i^2)}{2\sigma_s^2} \quad (7)$$

where σ_s is variance to the sides of the human ($\theta_i \pm \frac{\pi}{2}$) and σ is the variance in the direction of the human orientation.

We understand that personal space distances depend on many factors, including cultural differences, the environment, or a pedestrian's personality. Hence we have modeled the personal space distances as an adaptive Gaussian function that is dynamically updated by our navigation pipeline (detailed in section 3.4).

3.4. Intent-Aware Navigation

Our navigation framework is defined as a policy network trained to reach the goal-point while adjusting to the obstacles and personal space constraints of the humans. Three consecutive LiDAR scans from the robot are processed to accommodate our adaptive proxemic constraints for each detected human. Our policy network is inspired from [39, 12]. Our policy network receives the processed LiDAR scans and the intent-aware trajectory predictions for each human and outputs probabilities over the action space considered for the navigation task.

Action Space: The action space is a continuous set of permissible velocities. The action of the robot includes the translational and rotational velocity. To accomodate the robot kinematics, we set the bounds for transational velocity, $v \in [0.0, 1.0]$ and rotational velocity, $w \in [-1.0, 1.0]$. We sample actions at step t using equation 8

$$a_t = \pi(l_0, l_1, l_2, h_0, h_1, \dots, h_i) \quad (8)$$

where l_0, l_1, l_2 represent the three consecutive processed LiDAR scan frames and h_0, h_1, \dots, h_t represent the historical and predicted human trajectories concatenated together.

Policy Network: The policy network has four components $\{f_{traj}, f_{enc}, f_{act}\}$ (depicted in figure 3). f_{traj} is for encoding the human trajectories. We embed the concatenated (historical & predicted) trajectories to skeletal gait to image embedding in [25], resize them to 244×244 , and pass them to f_{traj} , which consists of four 5×5 Conv, Batch-Norm, ReLU. Each Conv block is followed by a 2×2 Max-Pool blocks, producing an encoded image of human trajectories $z_t^{img} = f_{traj}([h_0, h_1, h_i])$

The three consecutive lidar frames are passed through two 1×1 Conv, followed by a 256D fully-connected (FC) layer. The lidar frames are encoded as $z_t^{lidar} = f_{enc}([l_0, l_1, l_2])$. The f_{act} is a multi-layer perceptron (MLP)

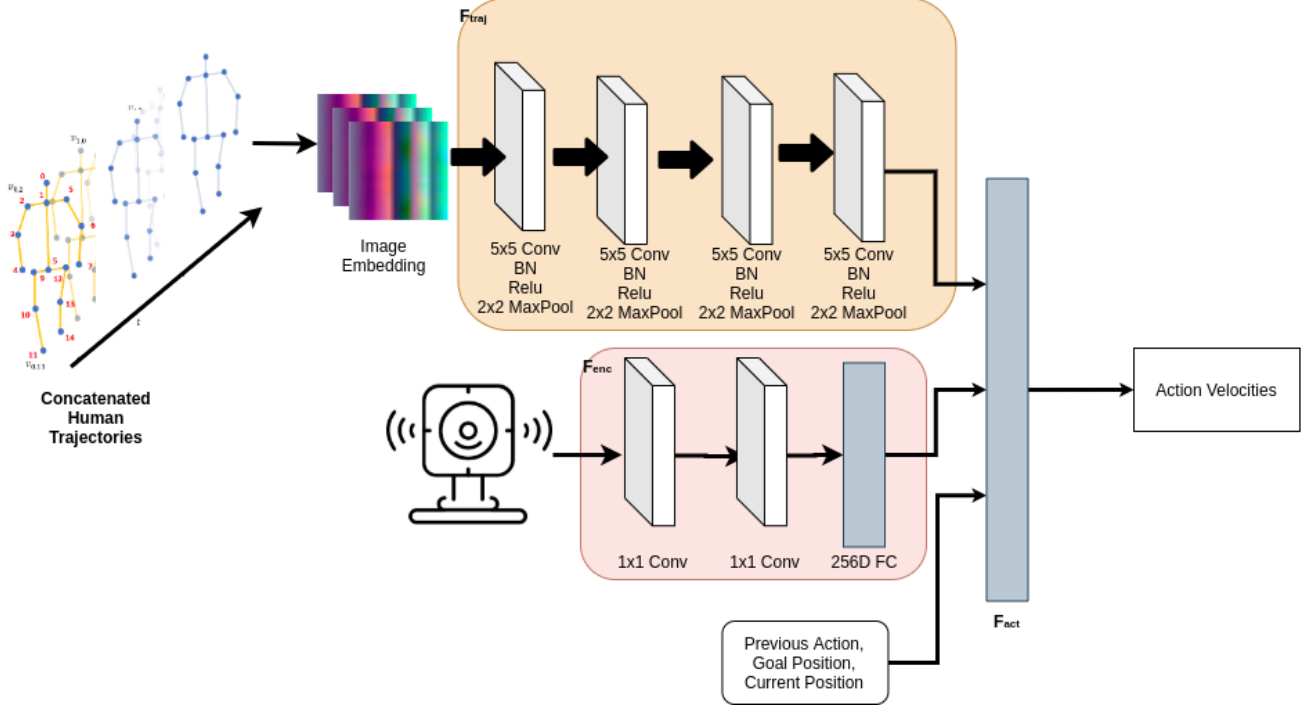


Figure 3. Our Navigation pipeline takes in the intent-aware human trajectories, LiDAR scans and Robot’s positional information as input to a policy networks. The policy network outputs the *robot velocity vectors* as action space.

network, with 1 128D FC hidden layer and finally produces the action velocities. f_{act} takes in the encoded human trajectories, z_t^{img} , lidar encodings, z_t^{lidar} , previous velocity, v_{t-1} , goal position, s_g , and current robot position, s_t , to predict the robot velocities at time t , given by equation 9.

$$[h]v_t = f_{act}([z_t^{img}, z_t^{lidar}, v_{t-1}, s_g, s_t]) \quad (9)$$

v_t is then sent to a linear layer with softmax to derive the probability distribution over the action space, from which the action is sampled. We learn $\{f_{traj}, f_{enc}, f_{act}\}$ via reinforcement learning.

Rewards: Our reward function for the policy network is inspired from [12]. Our goal is to find a good strategy to avoid collisions during navigation, minimize the arrival time and avoid any negative impact on the humans while navigating, i.e., avoid human emotions progressing into *Angry*, *Sad* while navigating (unless respective humans already display negative emotions). The reward function to achieve the mentioned goals is given in equation 10

$$r^t = r_g^t + r_c^t + r_w^t + r_e^t \quad (10)$$

The reward r at time t is a combination of reward for reaching goal, r_g , reward for avoid collisions, r_c , reward for smooth movement, r_w and reward for avoid negative impact on humans, r_e . The reward for reaching intended goal/target is given by equation 11.

$$r_g^t = \begin{cases} r_{arrival}, & \text{if } \|p^t - g\| < \xi. \\ w_g(\|p^{t-1} - g\| - \|p^t - g\|), & \text{Otherwise.} \end{cases} \quad (11)$$

The penalty for colliding with obstacles is given by equation 12.

$$r_c^t = \begin{cases} r_{collision}, & \text{if robot collides.} \\ 0, & \text{Otherwise.} \end{cases} \quad (12)$$

For ensuring smooth navigation, the penalty for large rotational velocities is given by equation 13.

$$r_w^t = \begin{cases} w_w|w^t|, & \text{if } |w^t| > 0.7. \\ 0, & \text{Otherwise.} \end{cases} \quad (13)$$

To ensure the robot does not alarm any pedestrian, we penalize the robot for any change in detected human emotion into negative emotions, *Angry*, *Sad*, with equation 14. The penalty is only applied when the human emotion, e_i , changes from non-negative emotion to negative emotions. In other words, we do not penalize the robot when human emotion remains unchanged.

$$r_e^t = \begin{cases} r_e, & \text{if } e_0, \dots, e_i \in \{Angry, Sad\}. \\ 0, & \text{Otherwise.} \end{cases} \quad (14)$$

In our implementation, we use $r_{arrival} = 15, w_g = 2.5, r_{collision} = -15, w_w = -0.1, r_e = -2.5, \xi = 0.1$

4. Experiments and Results

4.1. Human Intent Prediction

4.1.1 Metric

?? Since our human intent prediction is modeled as a trajectory prediction module, we evaluate the network with metrics commonly used for full-body trajectory/pose prediction networks. We the average l_2 distance between the ground-truth and the predicted poses at each time step for all humans present in the frame, aka, **MSE** as the metric.

4.1.2 Datasets

In this work, we use datasets specially designed for different tasks.

Human Emotion Datasets: Our intent prediction system is reinforced with emotion labels extracted from the historical gaits. For this purpose, we use two labeled datasets by Randhavane et al. [29], and Bhattacharya et al. [5]. It contains 3D skeletal joints of 342 and 1835 human gait cycles each (2177 gait samples in total).

Human Intent Prediction Datasets: Our intent prediction system is modeled as a trajectory prediction system, based on historical trajectory/gait sequences reinforced with human emotions for the same. We use two social datasets, created from NTU RGB+D 60 [34] and PoseTrack [2] for training and evaluating our and demonstrate its superior performance against several relevant baselines. The NTU dataset contains both single person actions and mutual actions. The PoseTrack is a large-scale multi-person dataset based on the MPII Multi-Person benchmark. The dataset covers a diverse variety of interactions, including person-person and person-object, in crowded, dynamic scenarios. For our experiments, we consider only the actions involving human *walking and/or running*. Hence we only select samples that fall under these categories.

4.1.3 Implementation Details

For training, our dataset (4.1.2) has a train-validation split of 90%-10%. We perform training using an ADAM [16] optimizer, with decay parameters of ($\beta_1 = 0.9$ and $\beta_2 = 0.999$). The experiments were run with a learning rate of 0.009 and with 10% decay every 250 epochs. The models were trained with MSE loss, \mathcal{L} . The training was done on 2 Nvidia RTX 2080 Ti GPUs having 11GB of GPU memory each and 64 GB of RAM.

4.1.4 Analysis on Experiment Results

In Table 1, we compare the performance of our model with other state-of-the-art models for trajectory prediction. It can be seen that our model provides a marginal boost to the trajectory predictions. We also compare our model with [26] and tabulate our results in Table 1. We use Human3.6M [15] dataset for comparing with [26]. We also showcase the performance of our model with and without the Human Emotion Context 3.2.1. It can be clearly seen that our Human intent prediction system performs much better with the Human Emotion Context.

4.2. Intent-Aware Navigation

4.2.1 Metric

We evaluate our navigation pipeline using three metrics, (i) Total distance traveled from source to goal, (ii) Time taken to reach the goal, (iii) Average personal space deviation (Δ_{ps}^{avg}), i.e., the difference between expected personal space and actual personal space provided by the robot while passing the human averaged across all human encounters.

4.2.2 Implementation Details

We rely on simulation environments to train our policy network. We use Stage Mobile Robot Simulator to generate multiple scenarios (see in figure 4) with obstacles to train our policy network. To aid policy convergence, we perform a multi-stage training of our policy network. We initially train the network on random scenarios from figure 4 - (A), without any obstacles. The map is divided into 6×6 grid. A random point from two different grids are chosen as source and target locations for training the random policy. Once the robot converges with a policy to reach a goal without obstacles, we further train on random samples with obstacles. Sample maps are shown in figure 4 - (B to E). Finally, we train the robot with human proxemic constraints. Since modeling human gait trajectories in simulation environments is extremely complex, we randomly sample human emotions and trajectories for training our policy network. We use RMSProp [14] for training our policy network with learning rate 0.00004 and $\epsilon = 0.00005$.

4.2.3 Analysis on Experiment Results

We tabulate the results from our experiment in Table 2. We compare the our implementation with [12] and [38]. We use scenarios 5 and 6 from figure 4 to perform our comparison studies. We also perform 20 iterations of the testing for each scenario under multiple environmental configurations (initial and goal positions, number, and position of obstacles, human and emotion parameters). It can be seen that our

Method	NTU RGB+D 60 [34]			PoseTrack [2]		
	Millisecond			Millisecond		
	80	160	320	80	160	320
ZeroPose-ZeroMotion	153.3	252.5	433.5	15.1	21.5	35.8
ZeroPose-ConstantMotion	154.7	265.4	436.8	15.4	22.0	36.1
ConstantPose-ConstantMotion	155.2	272.4	442.5	16.1	22.3	36.3
LocalPose-ZeroMotion	75.2	115.4	216.3	14.9	21.6	35.3
LocalPose-ConstantMotion	72.4	114.6	215.8	14.7	20.8	34.7
<i>EWareNet</i> (ours)	42.5	107.2	203.7	12.6	14.5	19.7

Table 1. Comparison of *EWareNet* with various baselines on **MSE** metric. We can see that our *EWareNet* has the **best MSE** across all the timesteps in consideration.

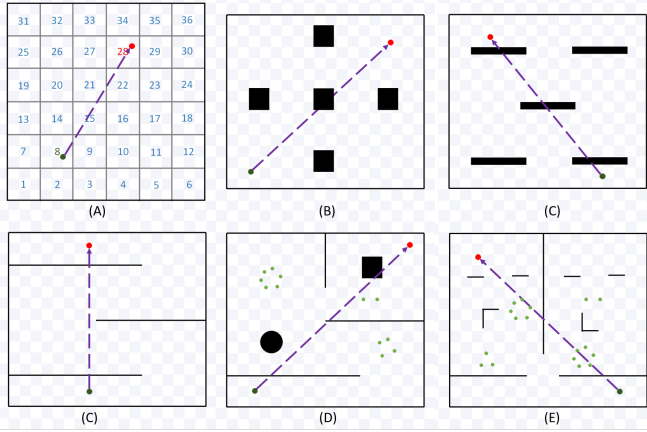


Figure 4. The various scenarios used to train our Navigation pipeline. As mentioned in section 4.2.2, several configurations of parameters within a scenario is tweaked to generated multiple training/testing scenarios based on figures A-E.

Method	Total Distance (m)	Avg. Time (min)	Δ_{ps}^{avg} (m)
Scenario 5			
Crowdmove [12]	152.5	2.6	25.3
RRT [38]	210.4	3.5	27.4
PRM [38]	217.6	3.6	26.8
Ours	172.3	2.9	10.2
Scenario 6			
Crowdmove [12]	224.5	7.2	57.8
RRT [38]	262.8	9.5	63.4
PRM [38]	245.6	8.7	61.8
Ours	237.6	8.7	32.8

Table 2. Comparison of *EWareNet* with various baselines using scenarios 5 and 6 from figure 4. We report the metrics mentioned in section 4.2.1 compared with [12] and [38]. We can see that our *EWareNet* has the **best Average personal space deviation** (Δ_{ps}^{avg}) across all our experiments.

implementation has the best Average Personal Space Deviation across all our experiments. Figure 5 showcases the experimental results of our comparison studies.

5. Conclusion

We introduce a novel approach using *transformers/recurrent networks* to predict the full-body human intent or behavior in the form of trajectory/gaits based on historical gait sequences, which drastically improves accuracy compared to SOTA. We also present a novel navigation planning algorithm based on deep reinforcement learning that takes into consideration the environment, human intent, and the robot’s reactionary impact on human behavior. Our method explicitly considers pedestrian behavior in crowds and the robot’s impact on the environment and the uncertainty in the robot’s sensor suite. Finally, we introduce an adaptive spatial density function to represent the proximal constraints for humans that captures humans’ unique personal comfort space in terms of pose, intent, and emotion.

References

- [1] Abulikemu Abuduweili, Siyan Li, and Changliu Liu. Adaptable human intention and trajectory prediction for human-robot collaboration. *arXiv preprint arXiv:1909.05089*, 2019. 2
- [2] M. Andriluka, U. Iqbal, E. Ensafutdinov, L. Pishchulin, A. Milan, J. Gall, and Schiele B. PoseTrack: A benchmark for human pose estimation and tracking. In *CVPR*, 2018. 7, 8
- [3] Aniket Bera, Tanmay Randhavane, and Dinesh Manocha. The emotionally intelligent robot: Improving socially-aware human prediction in crowded environments. In *Proceedings of the IEEE Conference on Computer Vision and Pattern Recognition Workshops*, 2019. 2, 3
- [4] A. Bera, T. Randhavane, R. Prinja, K. Kapsaskis, A. Wang, K. Gray, and D. Manocha. How are you feeling? multi-modal emotion learning for socially-assistive robot navigation. In *2020 15th IEEE International Conference on Automatic Face and Gesture Recognition (FG 2020) (FG)*, pages 894–901, 2020. 2
- [5] Uttaran Bhattacharya, Trisha Mittal, Rohan Chandra, Tanmay Randhavane, Aniket Bera, and Dinesh Manocha. Step: Spatial temporal graph convolutional networks for emotion perception from gaits. In *Proceedings of the Thirty-Fourth*

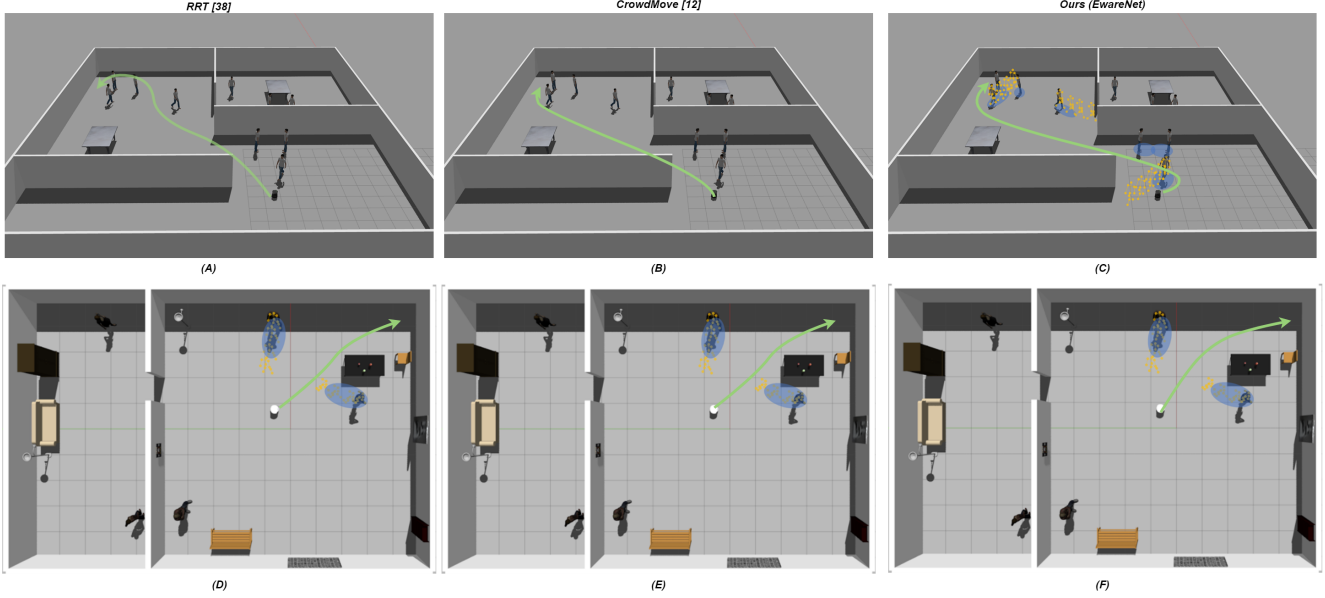


Figure 5. **Experimental Demo:** We showcase the performance of our *EWareNet* with other algorithms mentioned in Table 2. Here the trajectory taken by the robot is depicted in **Green**, along with intent-aware trajectories as gaits in **Yellow** and adaptive personal/comfort space area around human in **Blue**. Figures A & D represent the experiment with RRT [38], B & E represent experiment with CrowdMove [12] and C & F represents *EWareNet*.

- AAAI Conference on Artificial Intelligence, AAAI’20, page 1342–1350. AAAI Press, 2020. **7**
- [6] TB Brown, B Mann, N Ryder, M Subbiah, J Kaplan, P Dhariwal, A Neelakantan, P Shyam, G Sastry, A Askell, et al. Language models are few-shot learners. *arXiv preprint arXiv:2005.14165*. **4**
- [7] Carlos Busso, Zhigang Deng, Serdar Yildirim, Murtaza Bulut, Chul Min Lee, Abe Kazemzadeh, Sungbok Lee, Ulrich Neumann, and Shrikanth Narayanan. Analysis of emotion recognition using facial expressions, speech and multimodal information. In *ICMI*. ACM, 2004. **1**
- [8] Luca Caltagirone, Mauro Bellone, Lennart Svensson, and Mattias Wahde. Lidar–camera fusion for road detection using fully convolutional neural networks. *Robotics and Autonomous Systems*, 111:125 – 131, 2019. **3**
- [9] R Dabral, A Mundhada, et al. Learning 3d human pose from structure and motion. In *ECCV*, 2018. **3**
- [10] Jacob Devlin, Ming-Wei Chang, Kenton Lee, and Kristina Toutanova. Bert: Pre-training of deep bidirectional transformers for language understanding. *arXiv preprint arXiv:1810.04805*, 2018. **4**
- [11] Vishnu Sashank Dorbala, Arjun Srinivasan, and Aniket Bera. Can a robot trust you? a drl-based approach to trust-driven human-guided navigation. *arXiv preprint arXiv:2011.00554*, 2020. **2**
- [12] Tingxiang Fan, Xinjing Cheng, Jia Pan, Dinesh Manocha, and Ruigang Yang. Crowdmove: Autonomous mapless navigation in crowded scenarios. *arXiv preprint arXiv:1807.07870*, 2018. **5, 6, 7, 8, 9**
- [13] Francesco Giuliari, Irtiza Hasan, Marco Cristani, and Fabio Galasso. Transformer networks for trajectory forecasting. *arXiv preprint arXiv:2003.08111*, 2020. **4**
- [14] Geoffrey Hinton, Nitish Srivastava, and Kevin Swersky. Neural networks for machine learning lecture 6a overview of mini-batch gradient descent. *Cited on*, 14(8), 2012. **7**
- [15] Catalin Ionescu, Dragos Papava, Vlad Olaru, and Cristian Sminchisescu. Human3.6m: Large scale datasets and predictive methods for 3d human sensing in natural environments. *IEEE transactions on pattern analysis and machine intelligence*, 36(7):1325–1339, 2013. **7**
- [16] Diederik P Kingma and Jimmy Ba. Adam: A method for stochastic optimization. *arXiv preprint arXiv:1412.6980*, 2014. **7**
- [17] Rachel Kirby. Social robot navigation. 2010. **5**
- [18] A. Kleinsmith and N. Bianchi-Berthouze. Affective body expression perception and recognition: A survey. *IEEE Transactions on Affective Computing*, 4(1):15–33, Jan 2013. **1**
- [19] Thibault Kruse, Amit Kumar Pandey, Rachid Alami, and Alexandra Kirsch. Human-aware robot navigation: A survey. *Robotics and Autonomous Systems*, 61(12):1726 – 1743, 2013. **5**
- [20] Guangliang Li, Hamdi Dibeklioglu, Shimon Whiteson, and Hayley Hung. Facial feedback for reinforcement learning: A case study and offline analysis using the tamer framework, 2020. **3**
- [21] Bryan Lim, Serkan O Arik, Nicolas Loeff, and Tomas Pfister. Temporal fusion transformers for interpretable multi-horizon time series forecasting. *arXiv preprint arXiv:1912.09363*, 2019. **4**
- [22] Trisha Mittal, Uttaran Bhattacharya, Rohan Chandra, Aniket Bera, and Dinesh Manocha. M3er: Multiplicative multi-modal emotion recognition using facial, textual, and speech cues, 2019. **1**

- [23] Trisha Mittal, Pooja Guhan, Uttaran Bhattacharya, Rohan Chandra, Aniket Bera, and Dinesh Manocha. Emoticon: Context-aware multimodal emotion recognition using frege’s principle. In *Proceedings of the IEEE/CVF Conference on Computer Vision and Pattern Recognition*, pages 14234–14243, 2020. 1, 2
- [24] Abdullallah Mohamed, Kun Qian, Mohamed Elhoseiny, and Christian Claudel. Social-stgcn: A social spatio-temporal graph convolutional neural network for human trajectory prediction. In *Proceedings of the IEEE/CVF Conference on Computer Vision and Pattern Recognition*, pages 14424–14432, 2020. 2
- [25] Venkatraman Narayanan, Bala Murali Manoghar, Vishnu Sashank Dorbala, Dinesh Manocha, and Aniket Bera. Proximo: Gait-based emotion learning and multi-view proxemic fusion for socially-aware robot navigation. *IROS*, 2020. 1, 2, 3, 4, 5
- [26] Dario Pavllo, David Grangier, and Michael Auli. Quaternet: A quaternion-based recurrent model for human motion. 7
- [27] Dario Pavllo, David Grangier, and Michael Auli. Quaternet: A quaternion-based recurrent model for human motion. *arXiv preprint arXiv:1805.06485*, 2018. 2
- [28] Tanmay Randhavane, Aniket Bera, Kyra Kapsaskis, Uttaran Bhattacharya, Kurt Gray, and Dinesh Manocha. Identifying emotions from walking using affective and deep features. *arXiv preprint arXiv:1906.11884*, 2019. 2
- [29] T. Randhavane, U. Bhattacharya, K. Kapsaskis, K. Gray, A. Bera, and D. Manocha. Learning perceived emotion using affective and deep features for mental health applications. In *2019 ISMAR*, Oct 2019. 7
- [30] Tanmay Randhavane, Uttaran Bhattacharya, Kyra Kapsaskis, Kurt Gray, Aniket Bera, and Dinesh Manocha. The liar’s walk: Detecting deception with gait and gesture. *arXiv preprint arXiv:1912.06874*, 2019. 2
- [31] Amir Rasouli, Iuliia Kotseruba, Toni Kunic, and John K Tsotsos. Pie: A large-scale dataset and models for pedestrian intention estimation and trajectory prediction. In *Proceedings of the IEEE International Conference on Computer Vision*, pages 6262–6271, 2019. 2
- [32] Gennaro Ruggiero, Francesca Frassinetti, Yann Coello, Mariachiara Rapuano, Armando Schiano Di Cola, and Tina Iachini. The effect of facial expressions on peripersonal and interpersonal spaces. *Psychological research*, 2017. 5
- [33] Ariel Ruiz-Garcia, Mark Elshaw, Abdulrahman Altahhan, and Vasile Palade. Deep learning for emotion recognition in faces. In Alessandro E.P. Villa, Paolo Masulli, and Antonio Javier Pons Rivero, editors, *Artificial Neural Networks and Machine Learning*, pages 38–46, Cham, 2016. Springer International Publishing. 2
- [34] Amir Shahroudy, Jun Liu, Tian-Tsong Ng, and Gang Wang. Ntu rgb+d: A large scale dataset for 3d human activity analysis. In *IEEE Conference on Computer Vision and Pattern Recognition*, June 2016. 7, 8
- [35] Paweł Tarnowski, Marcin Kołodziej, Andrzej Majkowski, and Remigiusz J. Rak. Emotion recognition using facial expressions. *Procedia Computer Science*, 108:1175 – 1184, 2017. International Conference on Computational Science, ICCS 2017, 12-14 June 2017, Zurich, Switzerland. 2
- [36] A. Tawari and M. M. Trivedi. Speech emotion analysis in noisy real-world environment. In *2010 20th International Conference on Pattern Recognition*, pages 4605–4608, Aug 2010. 1
- [37] Tin Lay Nwe, Foo Say Wei, and L. C. De Silva. Speech based emotion classification. In *Proceedings of TENCON 2001*, Aug 2001. 1
- [38] Araceli Vega, Luis J. Manso, Douglas G. Macharet, Pablo Bustos, and Pedro Núñez. Socially aware robot navigation system in human-populated and interactive environments based on an adaptive spatial density function and space affordances. *Pattern Recognition Letters*, 118:72 – 84, 2019. Cooperative and Social Robots: Understanding Human Activities and Intentions. 2, 3, 5, 7, 8, 9
- [39] Jianwei Yang, Zhile Ren, Mingze Xu, Xinlei Chen, David Crandall, Devi Parikh, and Dhruv Batra. Embodied visual recognition. *arXiv preprint arXiv:1904.04404*, 2019. 5